Local deformation processes and damage evolution in MMCs

Klaus Unterweger, Otmar Kolednik

Erich Schmid Institute of Material Science, Austrian Academy of Sciences,
Jahnstrasse 12, A – 8700 Leoben

ABSTRACT

Particle reinforced MMCs with a particle size of 10µm and two different particle volume fractions are analyzed by the means of automatic local deformation analysis. The pure matrix material is also tested, and the results are compared to those of the MMCs. It is found that the material with 10% particles deforms similar to the matrix, whereas the deformation of the 20% material is different, as it is controlled by particle clusters. The crack tip opening displacements at particle failure sites and a typical shear band distance are determined.

KEYWORDS: metal matrix composite, composite architecture, digital image analysis, local deformation behavior, local fracture behavior

1. INTRODUCTION

Our current research project focuses on the local deformation, damage, and fracture behavior of particle reinforced metal matrix composites (MMCs). The interest lies especially on the influence of the local architectural parameters of the composite on the local deformation and damage behavior. We want to improve the understanding of the mechanisms that cause the poor ductility and fracture toughness of particulate reinforced MMCs, see, e.g., [1-4]. In order to get detailed information about the deformation behavior, individual regions on the surface of MMC tensile specimens are investigated by in-situ deformation experiments in the scanning electron microscope (SEM).

The SEM images that are captured at different stages of deformation are analyzed by the means of a system for digital image analysis in order to calculate maps of in-plane strains. This method was developed first by Davidson [5], who also performed first investigations on MMCs [6, 7]. We apply a new analysis system that provides a better accuracy and a higher lateral resolution [8, 9]. The development of strain localization and damage evolution by particle fracture and particle/matrix decohesion are monitored and studied in detail. Some results have already been published, see. e.g. [9,10]

2. MATERIALS AND SPECIMENS

The investigated MMCs were powder-metallurgically processed. The matrix is an Al-6061 alloy and the reinforcing SiC particles have a mean diameter of d_p=10 µm. The volume fractions of the particles are f_v=10 and 20%, respectively.

The tensile specimens for the in-situ tests were cut perpendicularly to the extrusion axis of the material. They have a cross section of 2 x 2 mm and a gauge length of 8 mm. The specimens were slightly notched at the bottom face (opposite side to the measurement face) with a radius of approximately 20mm and a depth of 0.1mm, in order to locate the zone of deformation. The heat treatment was carried out after the machining of the specimens. The material was solution annealed at 530 °C for one hour, quenched in water (20 °C), and aged at 175 °C for 200 hours, which corresponds to an over-aged condition. The samples were mechanically polished. Chemically etching was not applied, in order to avoid distortions (e.g. etching grooves) at the matrix particle interface.

3. EXPERIMENTAL

During the in-situ tensile tests in the SEM, each specimen is loaded in discrete steps. At the different stages of deformation, global stress and strain data is recorded and SEM-micrographs are taken. The "global" strain ($\bar{\varepsilon}_{xx}$) is measured with the help of the SEM micrographs, by determining the average value of the deformation in the loading direction within the analyzed region

$$\bar{\varepsilon}_{xx} = \frac{1}{N_x \cdot N_y} \cdot \sum_{i=1}^{N_y} \sum_{j=1}^{N_x} \varepsilon_{xx}(i,j) .$$

Where N_x, N_y are the grid-sizes in x-, and y-direction, respectively. The analyzed regions have a size of about 160 x 128 µm and are captured by micrographs that have a resolution of 4000 x 3200 pixel. The loading direction is parallel to the horizontal axis (x).

The automatic local deformation analysis is based on the automatic detection of physically identical points on the specimen surface in two micrographs of the same specimen area. These points are called homologue points. The homologue points can be detected with an accuracy of approximately 0.05 pixel [4]. The density of the homologue points lies between 3 and 6 points per 100 pixel, i.e., 380.000 to 740.000 homologue points are found in each pair of micrographs.

Due to the fact that the micrographs are taken at different stages of deformation, each pair of homologue points defines a displacement vector. From the smoothed displacement field, the in-plane strain and rotation fields can be derived in a numerical way. The procedure is described in [8, 9]. The strain accuracy depends on the density of homologue points, the smoothing procedure, and the magnification of the micrographs [8]; for the current analysis, the strain accuracy was about $\Delta\varepsilon_{xx} \approx 0.01$ at a lateral resolution of 0.5 µm. In the current maps, we plot the relative strain in loading direction ($\tilde{\varepsilon}_{xx}$) that is the local strain in loading direction (ε_{xx}), divided by the global strain in the analyzed area ($\bar{\varepsilon}_{xx}$),

$$\tilde{\varepsilon}_{xx} = \frac{\varepsilon_{xx}}{\bar{\varepsilon}_{xx}} .$$

Due to the high Young's modulus of the SiC particles, the local strains in the SiC particles are below the measurement accuracy.

In order to estimate characteristic parameters for the deformation field, Fast-Fourier-Transformation technique was employed. With the help of this tool it is, for example, possible to determine a typical shear band distance (δ_{sh}).

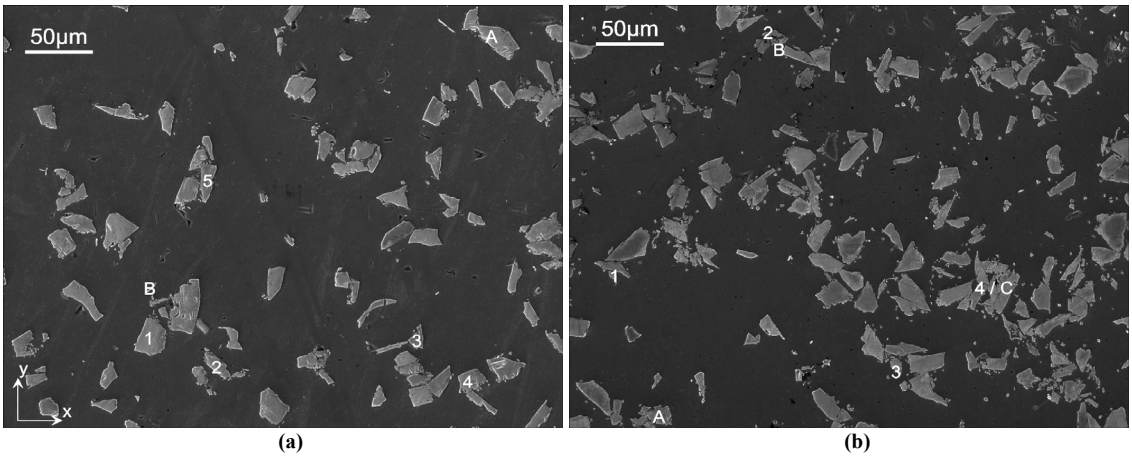

(a) (b)

Figure 1. SEM micrographs of the undeformed specimens. (a) MMC with f_v=10%, (b) MMC with f_v=20%. The loading direction is parallel to the horizontal axis (x).

4. RESULTS

In this section we discuss the results of three tensile experiments carried out with pure matrix material and the MMCs with 10 resp. 20% particle volume fraction. All three experiments were performed with the same SEM conditions (acceleration voltage, working distance, apertures), and an identical way of data processing was applied.

4.1 Matrix material

The matrix material without particles was tested in order to compare the deformation behavior of the matrix with those of the reinforced materials. In Figure 2 a collection of strain maps is shown. Presented are the relative strains in tensile direction ($\widetilde{\varepsilon}_{xx}$). The maps are cumulative strain maps showing local relative strains at global strains of 1.0, 3.0, and 5.9%, compared to the undeformed specimen. It seen that the shear bands occur mostly at an angle of approximately 45-50° to the loading axis. The local relative strain shows values up to 2 within these shear bands. Between these deformation bands there are areas that show a significantly lower relative strain, about $\widetilde{\varepsilon}_{xx} \approx$ 0.25-0.50.

By comparing the deformation patterns of the three maps in Fig. 2, one can see that the archetypes of the strain fields stays almost the same, although the global strain in the sample area varies from 1.0% in (a) over 3.0% in (b) to 5.9% in (c). During the experiment, the active deformation bands do not change, no new bands are activated. The distribution of the relative strains remains constant with rising global strain, which means that the absolute strain is scaling in a linear way with the global strain. The typical shear band distance $\delta_{sh} \approx$ 30 µm, remains constant, also, see Table 1. The specimen fractured at a global strain of approximately 7%.

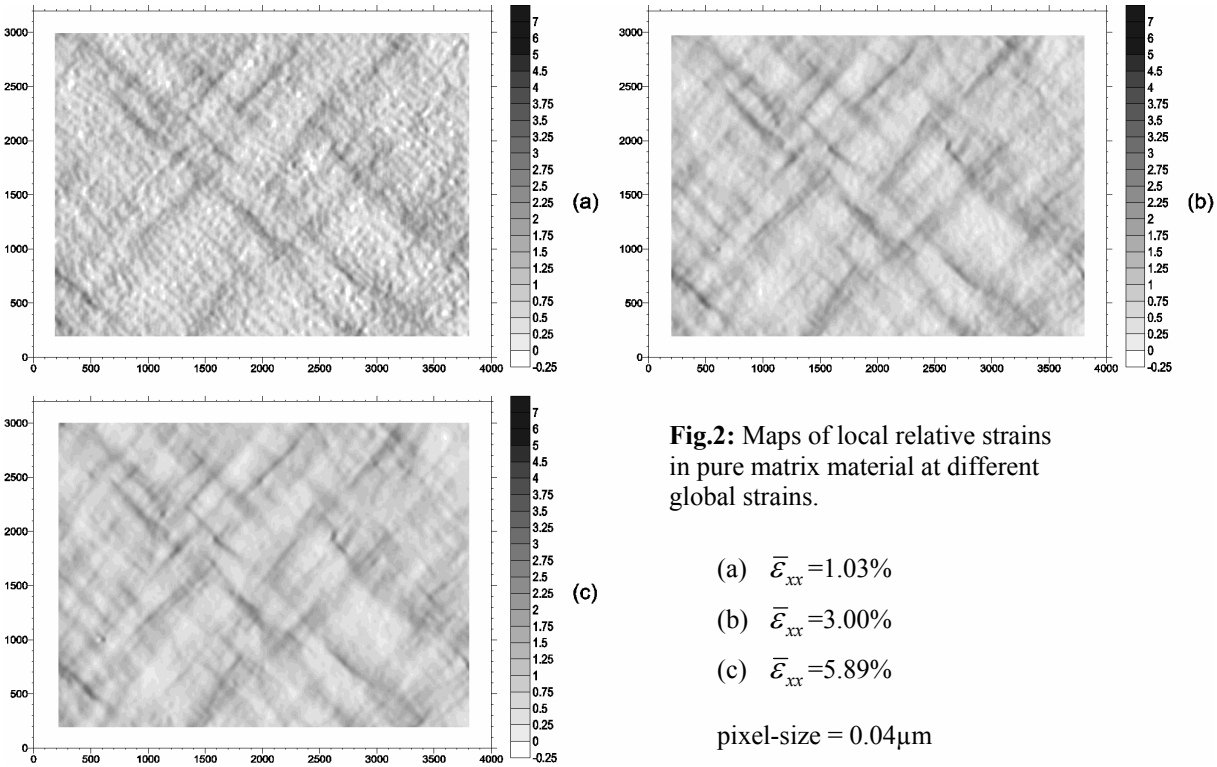

Fig.2: Maps of local relative strains in pure matrix material at different global strains.

(a) $\overline{\varepsilon}_{xx}$=1.03%

(b) $\overline{\varepsilon}_{xx}$=3.00%

(c) $\overline{\varepsilon}_{xx}$=5.89%

pixel-size = 0.04µm

Table 1: Shearband analysis

Matrix		MMC 10%		MMC 20%	
–		δ_p = 17.36µm*		δ_p = 13.78µm*	
$\bar{\varepsilon}_{xx}$	δ_{sh}	$\bar{\varepsilon}_{xx}$	δ_{sh}	$\bar{\varepsilon}_{xx}$	δ_{sh}
[%]	[µm]	[%]	[µm]	[%]	[µm]
1.03	32.1	1.50	24.3	0.93	41.8
3.00	29.3	3.04	24.5	1.42	48.5
5.89	31.0	6.28	25.2		

* δ_p is the theoretical particle distance, derived from a cubic primitive particle arrangement

4.2 MMC with 10% SiC particles

Figure 3 shows maps of relative strain ($\tilde{\varepsilon}_{xx}$) for the MMC with 10% particle content, during three stages of deformation, at 1.5, 3.0, and 6.3% global strain. These maps correspond to the specimen region depicted in Figure 1a.

The deformation behavior of the material is dominated by the formation of shear bands. These occur mostly at an angle of approximately 45° to the loading axis, and form in areas with a low particle content. Areas with higher particle content are usually evaded by shear bands. The local relative strain in the deformation bands reaches up to $\tilde{\varepsilon}_{xx} \approx$ 2.5. The areas between the shear bands containing no particles show relative strains in the range of 0.75-1. Only in the regions close to particles much lower strains between 0 and 0.25 are measured.

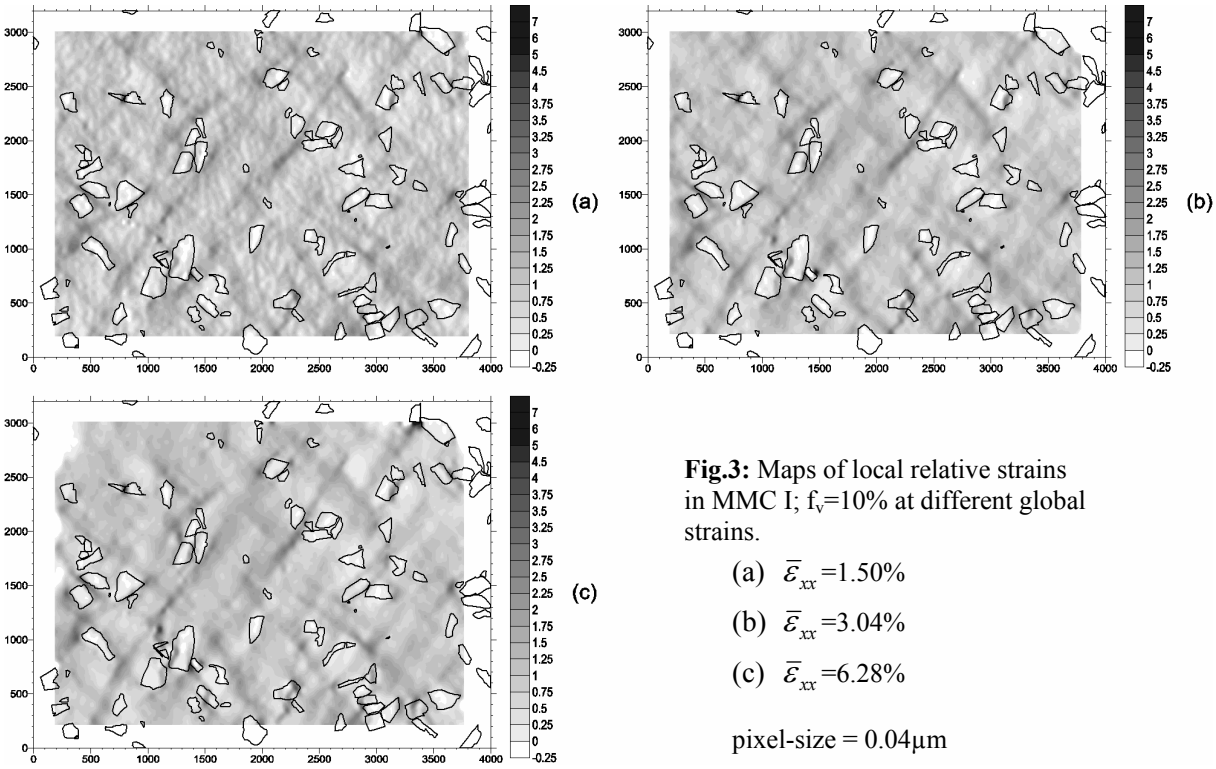

Fig.3: Maps of local relative strains in MMC I; f_v=10% at different global strains.

(a) $\bar{\varepsilon}_{xx}$=1.50%

(b) $\bar{\varepsilon}_{xx}$=3.04%

(c) $\bar{\varepsilon}_{xx}$=6.28%

pixel-size = 0.04µm

We find a matrix-like deformation behavior for this MMC: no formation of new shearbands and a linear scaling effect of the strain in the shear bands during the deformation of the material. The typical shear band distance $\delta_{sh} \approx$ 25 µm was found to be slightly smaller than in the matrix, but it remains constant during deformation, see Table 1. δ_{sh} is in the same range

as the theoretical particle distance. Along with a good particle distribution with low clustering, this is an indicator for a "homogeneous" deformation behavior.
It was reported in [9, 10] that for large particles (d_p=100µm) the fracture of single particles strongly influences the formation of shear bands in the matrix. In the actual experiment with the small particles, we do not find such a behavior. Even though several particles have already fractured at 6.3% (Fig. 2c), the shear band pattern has not changed significantly.
Figure 4 shows examples of particle failure sites. The micrographs show the cracks in the particles 2, 3, and 4, which are also indicated in Fig 1a. Confirm Table 2, where COD-values (crack tip opening displacement) for some fractured particles are shown. The COD_f-values (fractured particles) vary in the range from 0.1 to 0.5 µm at a global strain of 6.3%. Sites of matrix/particle decohesions are indicated alpha numerically in Fig. 1a. In Table 2 also COD_d values for matrix-particle decohesions are given, witch are in the range of 0.5µm at the same average strain. Compared with the COD values reported in [10] for an MMC with 100µm large particles, the actual COD-values are about one order of magnitude lower. We conclude that these small COD-values are too low to induce the formation of new shear bands in the matrix. Hence, the damage evolution does not primarily influence the deformation pattern in the investigated stages of deformation. The final frature of the specimen occurred at a global strain of about 7%. All in all, the local deformation behavior of the MMC with 10% SiC particles is very similar to those of the pure matrix.

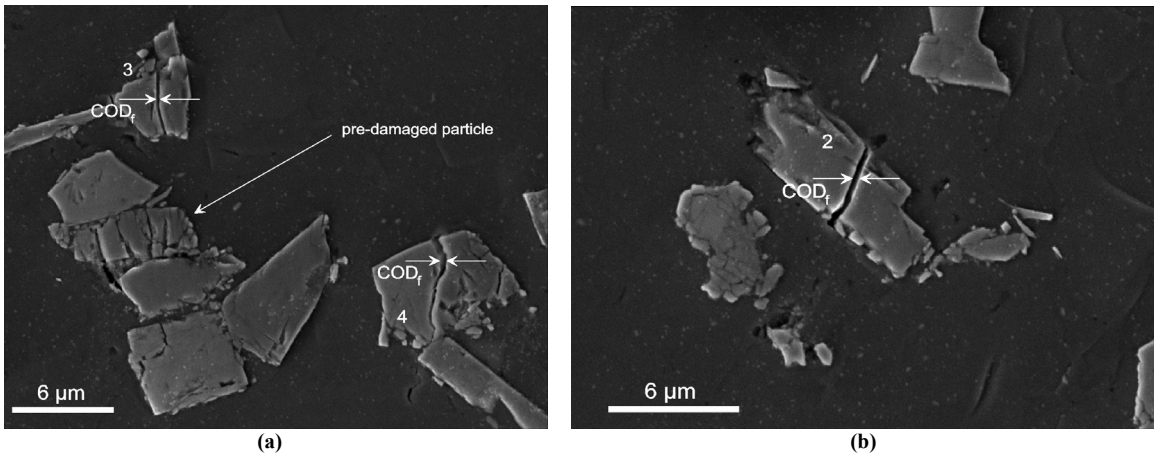

(a) (b)

Fig 4: Micrographs of particle failure sites in the deformed MMC specimen containing 10% particles. Depicted are details from Fig. 1a, at a strain of 6.28%.
(a) region 3/4, (b) region 2, compare Table 2 for COD values.

Table 2: Crack-tip-opening displacements at particles failure sites

MMC 10%				**MMC 20%**			
particle fracture		decohesion		particle fracture		decohesion	
particle	COD_f	particle	COD_d	particle	COD_f	particle	COD_d
[-]	[µm]	[-]	[µm]	[-]	[µm]	[-]	[µm]
1	0.08	A	0.56	1	0.08	A	0.20
2	0.28	B	0.60	2	0.16	B	0.28
3	0.20			3	0.17		
4	0.36			4	0.42	C	0.42
5	0.12						

Since the final fracture of the specimen occurred considerably far away from the analyzed area, we could not analyze the deformation and damage processes in the area of specimen failure. The fracture surface shows a high amount of fractured particles, thus it is clear that for the fracture process particle cracking is an important damage mechanism.

4.3 MMC with 20% SiC particles

Figure 5 shows two maps of local relative strains ($\widetilde{\varepsilon}_{xx}$) at 1.0 and 1.4% global strain for the MMC specimen containing 20% reinforcements. The maps correspond to the area depicted in Figure 1b.

The particle distribution in this specimen is dominated by reinforcement clusters (see also Fig 1b). The strain maps show a strong deformation band heading from the cluster 4/C in the middle lower right towards north-west to cluster 2/B. This deformation band is very dominant compared to the overall-deformation of the analyzed area and shows local relative strains up to 4. The origin of this shear band is a pre-damaged particle in the cluster 4/C. In this case, although the COD value at particle 4 is not high, the damage of the particle is the reason for the formation of a shear band that dominates the deformation in the analyzed area of the specimen. Areas with low particle content show relative strains of 1.5-2, which is higher than case of the MMC with 10% particles, and a result of the higher particle content. The typical shear band distance is $\delta_{sh} \approx$ 41-48µm which is much higher than in the matrix and also about 3 times higher than the theoretical particle distance, hence, this is a further indicator for a cluster controlled, very inhomogeneous deformation behavior.

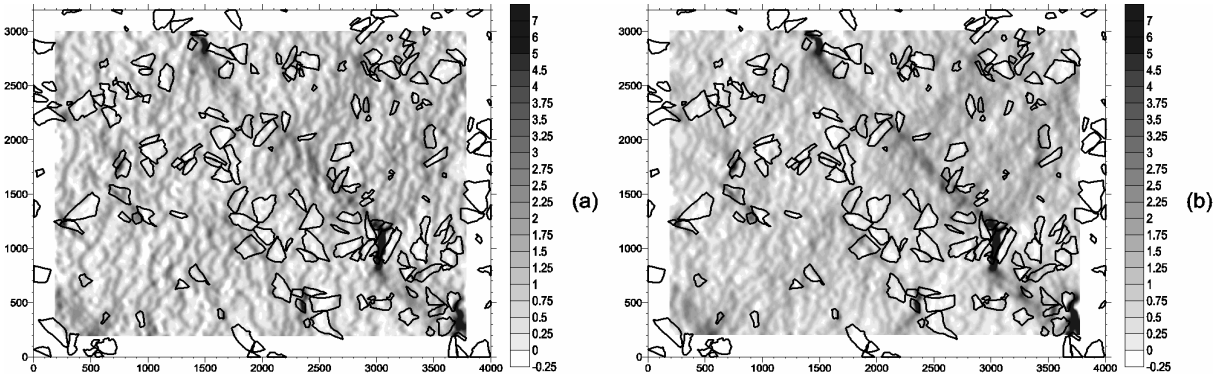

Fig 5: Maps of local relative strains in MMC II; f_v=20% at different global strains.
(a) at at $\overline{\varepsilon}_{xx}$=0.93%, (b) at $\overline{\varepsilon}_{xx}$=1.42%. pixel-size = 0.04µm

Figure 6 shows micrographs of the areas indicated as cluster 4/C and 2/B in Fig. 1b. The failure site at cluster 4/C shows debonding at particle C and the fractured particle 4, in this case the COD values are indentical, cf. Table 2. The measured COD values are in the range of 0.2µm for fractured particles and about 0.3µm for decohesions. These values are in the same range as for the specimen with 10% particles, although the average strain of the two specimens differ by a factor of 4.

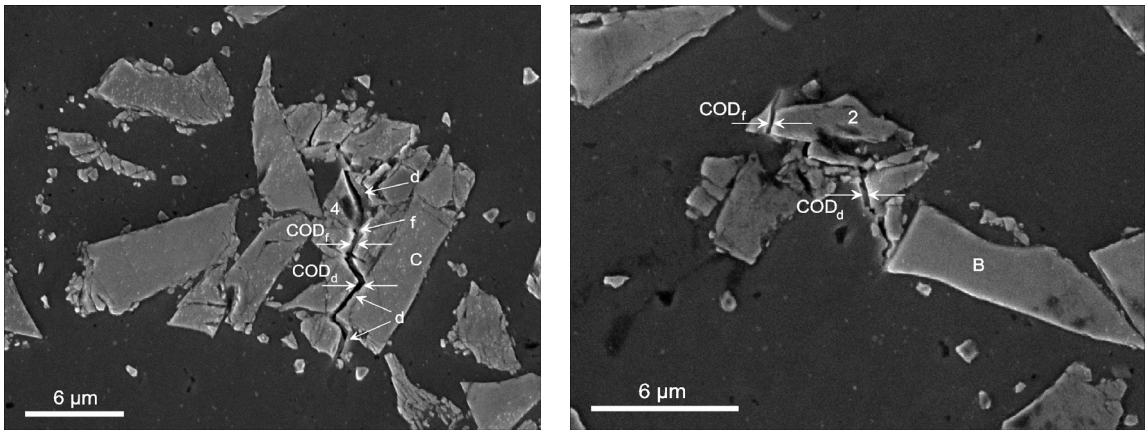

Fig 6: Micrographs of particle failure sites in the deformed MMC specimen containing 20% particles. Depicted are details from Fig. 1b, at a strain of 1.42%. Note the low CODs.
(a) region 4/C, (b) region 2/B; compare Table 2 for COD values; d...debonding, f...fracture

Another significant difference is that in the case of the higher particle content, these failures lead to the formation of one dominant shear band. We assume that the reasons therefore are, on the one hand, the by far stiffer behavior of the composite, due to the higher particle content, and, on the other hand, the clustered arrangement of the particles. The specimen fractured shortly after the deformation stage of $\bar{\varepsilon}_{xx}$ = 1.4%. We conclude that the deformation of the material with 20% particle content is controlled by the clustered arrangement of the reinforcements.

5. CONCLUSIONS

The local deformation behavior of the MMC with 10% SiC particles (d_p=10µm) is very similar to the local deformation behaviour of the matrix. Main damage mechanisms are particle fracture and matrix-particle decohesion. In the investigated regime of deformation (up to 6%), these failures do not influence the deformation behaviour significantly. The distance of the shear bands is only slightly smaller than in the matrix and in the range of the theoretical particle distance.

The MMC with 20% particle content behaves in a different way, because the clustered particle arrangement causes very inhomogeneous local deformations that lead to early fracture of the material. Particle fracture and decohesion occurred less frequently, but determine the deformation by allowing the matrix to deform locally. Failure sites occur mainly at particle clusters. The distance of the deformation bands is about three times higher than the theoretical particle distance and nearly 1.5 times higher than in the matrix, which is a result of the clustered particle arrangement and the localization of the deformation.

ACKNOWLEDGEMENTS

The authors acknowledge gratefully the financial support of this work by the Fonds zu Förderung der wissenschaftlichen Forschung under the project number P14333-PHY.

References:

1. Clyne, T. W. and Withers, P. J., *An introduction to metal matrix composites*, Cambridge Univiversity Press, GB, 1993.
2. Suresh, S., Mortensen, A. and Needleman, A., *Fundamentals of Metal Matrix Composites*, Butterworth - Heinemann, USA, 1993.
3. Pandey, A. B., Majumdar, B. S. and Miracle D. B., *Metallurgical and Materials Transactions,* **A 31A** (2000) 921-936
4. Majumdar, B. S. and Pandey, A. B., *Metallurgical and Materials Transactions,* **A 31A** (2000) 937-950
5. Davidson, D.L, *Scanning Electron Microscopy* 11 (1979) 79-81.
6. Davidson, D.L., *Metallurgical Transactions* **A 22** (1991) 113-123.
7. Davidson, D.L., *Metallurgical Transactions* **A 22** (1991) 97-112.
8. Tatschl, A. and Kolednik, O., *Materials Science and Engineering* **A 339** (2003) 265-280.
9. Unterweger, K., Dick, Th., Kolednik, O. and Pippan, R., *Non-linear mechanics of anisotropic materials, Proceedings of the 6th European Mechanics of Materials Conference (EMMC6)*, S. Cescotto, Ed., pp. 145-152, EUROMECH-MECAMAT, Liege, Belgium, 2002.
10. Unterweger, K., Kolednik, O., Pippan, R., *Proceedings of the 14th International Conference of Composite Materials (ICCM14)*, San Diego, USA, 2003.